Mansour *et al. Cancer Nanotechnology* (2023) 14:14
https://doi.org/10.1186/s12645-023-00163-0

Cancer Nanotechnology

RESEARCH Open Access

Targeted therapy for HCC using dumbbell-like nanoparticles conjugated to monoclonal antibodies against VEGF and cancer stem cell receptors in mice

Wafaa Mansour[1], Shahira Fathy EL Fedawy[2], Shimaa Attia Atta[1], Rewan Mohsen Zarie[1*], Nermeen Tayseer Aly Fouad[2], Sara Maher[1], Taghreed M. Hussein[3], Doaa Mohamed Abdel Aziz[2] and Manal Kamel[1]

*Correspondence: rewanmohsen@gmail.com

[1] Immunology Department, Theodor Bilharz Research Institute, Giza, Egypt
[2] Faculty of Medicine, Ain Shams University, Cairo, Egypt
[3] Physiology Department, National Organization for Drug Control and Research Pyramids Branch, Giza, Egypt

Abstract

Background: Hepatocellular carcinoma (HCC) is the leading cause of death worldwide. Nanoparticles allow early detection of tumor and delivery of chemotherapeutic drugs to the specific tumor site. This study aimed to assess the therapeutic role of dumbbell-like nanoparticles conjugated with monoclonal antibodies (mAbs) against both vascular endothelial growth factor (VEGF) and cluster of differentiation (CD) 90 (a cancer stem cell marker) in hepatocellular carcinoma experimental model. This study included 100 mice; HCC was induced chemically in 80 male Balb/c mice by diethylnitrosamine (DEN) and 20 mice served as normal control group. Mice were divided into four groups; pathological control group, mAbs-conjugated nanoparticles-treated group, nanoparticles (alone)-treated group and Avastin-treated group. Animals were sacrificed after one and two months of treatment for assessment of HCC response to treatment. Serum samples were collected and analyzed for alfa-feto protein (AFP), Caspase-3, VEGF-A by enzyme-linked immunosorbent assay (ELISA) technique and alanine transaminase (ALT) and aspartate transaminase (AST) by automated analyzer. Liver sections of sacrificed animals were stained with hematoxylin and eosin (H&E) for histopathological assessment.

Results: There were highly significant and significant differences (p value < 0.1 and < 0.5) between mAbs-conjugated nanoparticles-treated group and Avastin group, respectively, in comparison to pathological group. Both groups showed a significant decrease in all serum parameters, but mAbs-conjugated nanoparticles-treated group had more potent improvement effect when compared with Avastin group. MAbs-conjugated nanoparticles-treated group also showed the best improvement in liver architecture.

Conclusion: Dumbbell-like nanoparticles conjugated to anti-CD90 and Avastin is a novel therapeutic tool for HCC to target cancer stem cells and endothelial cells in the niche of the tumor.

Keywords: Hepatocellular carcinoma, Nanoparticles, Avastin, CD90

Background

Hepatocellular carcinoma (HCC) is the most common type of primary liver cancer in adults, and is the most common cause of death in people with cirrhosis (Tapper and

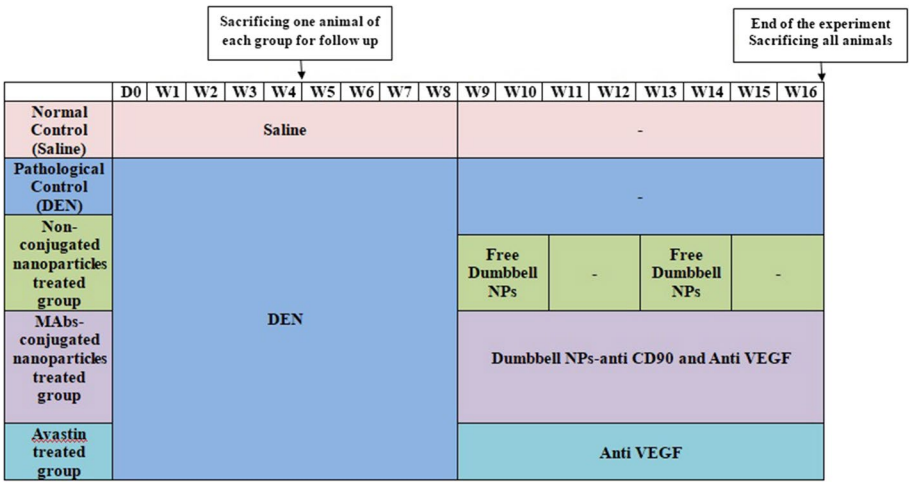

Scheme 1 A scheme of the experimental design

Parikh 2018). It represents up 75–85% of all primary liver cancers (Bray et al. 2018) and develops on a background of chronic liver disease, with hepatitis B virus (HBV) infection, hepatitis C virus (HCV) infection, alcohol abuse and nonalcoholic fatty liver disease being the major etiologies (Craig et al. 2019). Its diagnosis is usually late, and the survival rate is approximately 6 to 20 months (El-Serag 2011; Manghisi et al. 1998). Although the gold standard line of treatment is surgery, not all patients are eligible because of tumor stage or liver dysfunction. No new treatments for HCC have been approved. The lack of a curative pharmacological therapies for HCC, clarifies the utmost need for novel methods for better prognosis of HCC Scheme 1.

Cancer stem cells (CSCs) are a group of dividing cells with highly tumorigenic activity and remarkable resistance to conventional lines of treatment (Alkatout et al. 2008; Liu et al. 2006). CD90 is an important prognostic marker and effective therapeutic target for the treatment of hepatic cancers. This marker is used to identify potential hepatic CSCs from tumor specimens and blood samples of liver cancer patients (Hong et al. 2015).

It is well known that tumor cells secrete various growth factors, including vascular endothelial growth factor (VEGF), which triggers endothelial cells to form new capillaries and enhances the angiogenesis process. Bevacizumab (Avastin), is a recombinant humanized immunoglobulin G (IgG) monoclonal antibody that targets VEGF-A inhibiting the formation of the VEGF-A—vascular endothelial growth factor receptor-1 and 2 (VEGFR-1&2) complex; thus, restricting the tumor mass and reducing the possibility of metastases (Braghiroli et al. 2012).

Nanotherapeutics usage in drug delivery applications has recently increased because of their desirable therapeutic characteristics, such as prolonged systemic circulation and targeted drug delivery. These characters are particularly advantageous for cancer therapeutics because they would result in improved anticancer drugs efficacy and would

minimize the systemic toxicity (d'Angelo et al. 2010; Eskens and Verweij 2006; Heddleston et al. 2010).

Nanoparticles (NPs) conjugated to monoclonal antibodies and their fragments have remarkable impacts on personalized medicine. These particles provide specific internalization and accumulation in the tumor microenvironment (Kadkhoda et al. 2021).

Dumbbell-like nanoparticles (DBNPs) are referred to those particles with two different functional NPs in intimate contact that offers a controlled multifunctionality structure which allows conjugation with more than one therapeutic agent (Akbarzadeh et al. 2012; Gu et al. 2005).

In this study, we have designed DBNPs (iron and gold nanoparticles) where iron was tagged with VEGF monoclonal antibodies (mAbs) while gold was tagged with mAb against cancer stem cell marker (CD90). Both iron and gold are stable and nontoxic. Application of this novel mAbs-conjugated nanosystem showed interesting results revealing its promising application as an effective anticancer therapeutic drug delivery system.

Results

Synthesis and characterization of dumbbell-like Au-Fe_3O_4 nanoparticles

The size and morphology of gold (8 nm) and dumbbell-like Au-Fe_3O_4 nanoparticles (8–20-nm) (core−particle diameter) were checked by transmission electron microscopy (TEM). Avastin was linked to the Fe_3O_4 surface through polyethylene glycol (PEG, Mr = 3000), while CD90 was noncovalent conjugated to Au moiety of the dumbbell nanosystem (Fig. 1).

In vitro drug release

Drug release behavior of Avastin−Au-Fe_3O_4nanosystem was tested at two different pH values: pH 7.4, which mimics the pH of the blood stream and pH 5, which mimics the pH of the endosomes within cancer cells. In vitro release study results (Fig. 2) showed that Avastin−Au-Fe_3O_4 released more than 95% of Avastin at pH 5 over the period of 10 h. On the other hand, it required more than 16 h to reach the same percentage of release at pH 7.4.

Histopathological examination of liver specimens

Mice treated with dumbbell-like Au-Fe_3O_4 nanoparticles conjugated to bevacizumab (Avastin) and anti-CD90 monoclonal antibodies showed the best improvement of liver architecture and regression of tumor after one month of treatment when compared with Avastin and nano-treated groups, respectively. Avastin-treated group showed mild improvement in liver architecture after one month of treatment while a marked improvement was noticed after two months. The treatment with nonconjugated dumb bell-like Au-Fe_3O_4 nanoparticles showed the mildest improvement in liver architecture after two months when compared with mAbs-conjugated nanoparticles and Avastin-treated groups (Figs. 3, 4).

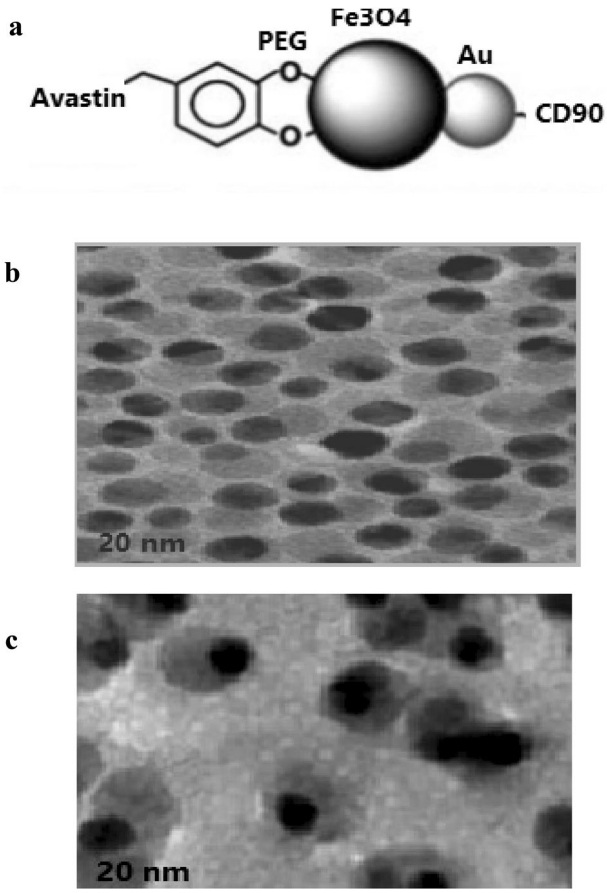

Fig. 1 Dumbbell-like Au-Fe_3O_4 nanoparticles. **a** Illustration of surface functionalization of the Au-Fe_3O_4 dumbbell- like nanoparticles. **b**, **c** TEM images of Au-Fe_3O_4 (8–20-nm) particles before **b** and after **c** surface modification

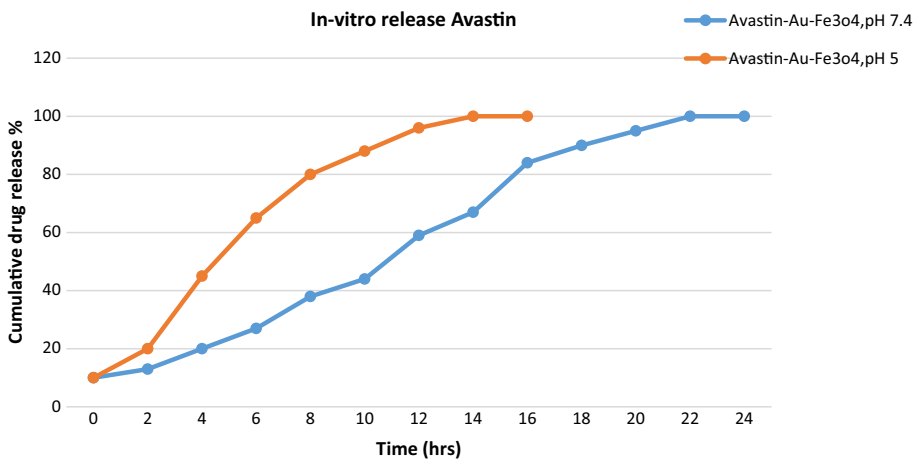

Fig. 2 *In vitro* release of Avastin from Avastin—Au-Fe_3O_4 nanosystem in PBS pH 7.4 and in Tris—HCl buffer pH 5

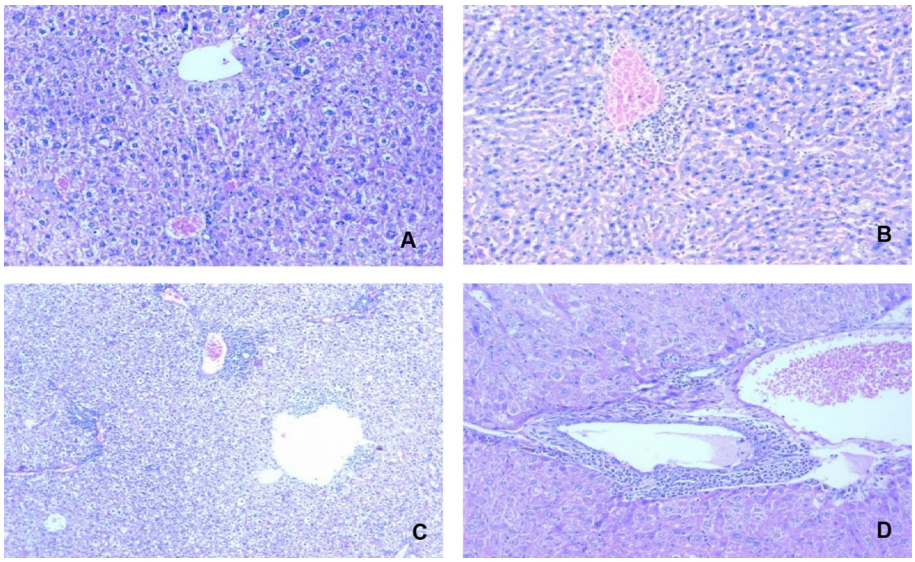

Fig. 3 Histopathological analysis of liver specimens of different groups after one month of treatment. **A** Pathological control group: showed marked disturbed liver architecture and marked polymorphism (H&E X10) **B** mAbs-conjugated nanoparticles-treated group: showed restoration of normal liver architecture, marked inflammatory infiltrate, mild polymorphism (H&E, 20X). **C** Avastin-treated group: showed moderate disturbed of liver architecture, moderate inflammatory infiltrate, mild increase mitosis, mild increase nuclear size and moderate polymorphism (H&E, 20X). **D** Nonconjugated nanoparticles-treated group: marked nodular and disturbed architecture, moderate inflammatory infiltrate, moderate increase mitosis, moderate increase nuclear size, bizarre shape of cells and marked polymorphism (H&E, 20X)

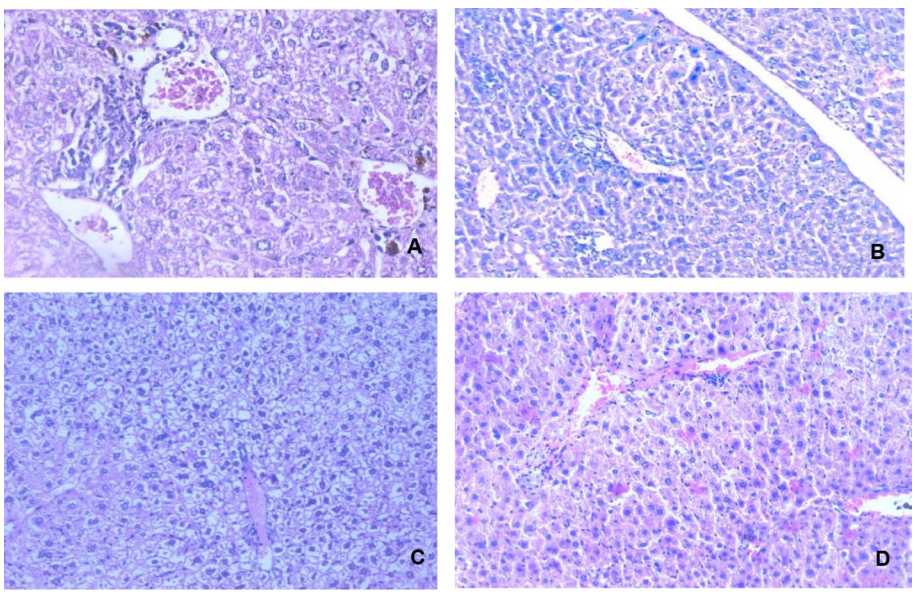

Fig. 4 Histopathological analysis of liver specimens of different groups after two months of treatment. **A** Pathological control group: showed marked disturbed liver architecture and marked polymorphism (H&E, X40) **B** mAbs-conjugated nanoparticles-treated group: showed preserved liver architecture, increased inflammatory reaction, mild polymorphism (anaplasia) (H&E, 20X). **C** Avastin-treated group: showed mild restoration of liver architecture, no inflammatory cells, clear cytoplasm and mild polymorphism (H&E, 20X). **D** Nonconjugated nanoparticles-treated group: showed moderate disturbed of liver architecture, decrease inflammation, moderate polymorphism (H&E, 20X)

Table 1 Mean significance ± SE values of serum levels of AFP, caspases-3, VEGF-A, ALT and AST levels in sera of different groups after first month of treatment

Animal groups (first month)	AFP ng/ml	ALT IU/ml	AST IU/ml	Caspases -3 ng/ml	VEGF-A pg/ml
Normal control	11.06 ± 0.12	99.04 ± 0.79	49.89 ± 2.44	3.37 ± 0.10	125 ± 0.19
Pathological control	55.14 ± 0.16[b]	306.8 ± 4.147[b]	131.1 ± 2.8[a]	4.94 ± 0.06[a]	249.9 ± 0.18[b]
mAbs-conjugated nanoparticles	22.09 ± 0.12[c]	130.6 ± 0.53[d]	61.17 ± 2.31[c]	32.11 ± 0.09[d]	140 ± 0.12[c]
Avastin	37.67 ± 0.21[e]	201.3 ± 0.51[e]	86.07 ± 1.49[e]	20.63 ± 0.23[e]	179.9 ± 0.15[e]
Nanoparticles	51.09 ± 0.15	279.6 ± 0.95	121.1 ± 1.93	5.45 ± 0.11	220.2 ± 0.14

[a] Significant and [b]high significant increase between pathological # normal groups ($P < 0.5$ and $P < 0.1$, respectively)

[c] Significant and [d]highly significant difference between nanoparticles conjugated # pathological control groups ($P < 0.5$ and $P < 0.1$, respectively)

[e] Significant and [f]highly significant difference between Avastin and pathological control groups ($P < 0.5$& $P < 0.1$, respectively)

[g] Significant in the mean values of different markers between first and second months

Table 2 Mean significance ± SE values of serum levels of AFP, caspases-3, VEGF-A, ALT and AST levels in sera of different groups after second month of treatment

Animal groups (second month)	AFP ng/ml	ALT IU/ml	AST IU/ml	Caspases-3 ng/ml	VEGF-A pg/ml
Normal control	11.06 ± 0.12	99.04 ± 0.79	49.89 ± 2.44	3.37 ± 0.10	125 ± 0.19
Pathological control	68.08 ± 0.14[b]	346.6 ± 2.23[b]	161.1 ± 5.24[b]	6.14 ± 0.09[b]	280.7 ± 0.36[b]
mAbs conjugated nanoparticles	13.15 ± 0.11[dg]	101.7 ± 2.41[dg]	44.9 ± 1.75[dg]	4.28 ± 0.19[eg]	125.5 ± 0.25[dg]
Avastin	25.10 ± 0.09[f]	158.2 ± 2.89[ea]	61.7 ± 1.88[e]	12.21 ± 0.15[e]	159.9 ± 0.12[e]
Nanoparticles	49.47 ± 0.19	270 ± 0.11	137.6 ± 2.50	7.42 ± 0.11	200.2 ± 0.12

[a] Significant and [b]high significant increase between pathological # normal groups ($P < 0.5$ and $P < 0.1$, respectively)

[c] Significant and [d]highly significant difference between nanoparticles conjugated # pathological control groups ($P < 0.5$& $P < 0.1$, respectively)

[e] Significant and [f]highly significant difference between Avastin and pathological control groups ($P < 0.5$ and $P < 0.1$, respectively)

[g] Significant in the mean values of different markers between first and second months

Biochemical analysis

MAbs-conjugated nanoparticles-treated group showed significant and highly significant improvement in the 2 months of treatment, where remarkable decrease in AFP, ALT, AST, and VEGF-A was detected when compared with pathological control after first (p value < 0.5) and second month (p value < 0.1), respectively. Moreover, mAbs-conjugated nanoparticles-treated group showed highly significant increase in caspases-3 when compared with pathological control after first month (p value < 0.1), while it showed significant decrease after second month treatment when compared with the pathological control (p value < 0.5). Avastin-treated group showed significant decrease in all parameters as well but showed significant increase in caspases-3 when compared with pathological control after first and second month (p value < 0.5).

The data of each parameter are illustrated in Tables 1 and 2.

Discussion

Different studies discussed and exhibited the promising role of dumbbell-like Au-Fe_3O_4 NPs as highly sensitive diagnostic and therapeutic nano-carriers (N. Yu et al. 2005). In this study, dumbbell-like Au − -Fe_3O_4 nanoparticles were synthesized and conjugated with monoclonal antibodies against VEGF-A (Avastin) and CD90 to target cancer stem cells of liver cancer. NPs size, surface functionalization and conjugation with monoclonal antibodies were checked and confirmed by TEM. Drug release is currently assessed using a variety of methods including sample and separate (SS), dialysis membrane (DM), continuous flow (CF), as well as voltametry and turbidimetry (D'Souza 2014). In our study, we used the dialysis membrane method. The *in vitro* drug release results confirmed that Avastin−Au-Fe_3O_4 exhibited faster release in pH5, which mimics the pH of endosomes within cancer cells, when compared with their release in pH 7.4. The pH-sensitivity property of Avastin−Au-Fe_3O_4 complex seems to be advantageous for cancer-targeted drug delivery because the acidic microenvironment of cancer cells facilitates active drug release from NPs, increases drug bioavailability to cancer cells, and leads to high therapeutic efficacy when compared with normal cells (Xu et al. 2008; Qi et al. 2010).

Our results showed that mAbs-conjugated nanoparticles-treated group had the best histopathological improvement where manifestations of anaplasia and metaplasia observed in pathological control were greatly reduced with restoration of normal liver architecture. Avastin-treated group showed mild disturbed liver architecture and moderate polymorphism when compared with pathological control. On the other hand, nonconjugated nanoparticles-treated group showed the least improvement when compared with pathological control with moderate nodular and disturbed architecture and marked polymorphism. These results are in agreement with several studies that discussed the improvement and antiangiogenic effect of metallic nanoparticles on induced HCC models (Baiga et al. 2019; Elaidy et al. 2017).

Our results also revealed that mAbs-conjugated dumbbell-like Fe_3O_4 nanoparticles-treated group showed a highly significant decrease in AFP, VEGF-A, ALT and AST levels in comparison with other groups. This significant decline indicates a promising and useful application of this therapeutic nanosystem to predict treatment response and survival in HCC patients.

Moreover, several studies confirmed the significant role of nanoparticles employment and induction of apoptosis in different cancer types (Baharara et al. 2016; Han et al. 2019; Nabin et al. 2021). In our study, caspase-3 level showed significant increase after one month of treatment with all of, mAbs-conjugated dumbbell-like Fe_3O_4 nanoparticles, Avastin group, or nanoparticles-treated group comparing to normal control. After two months of treatment, the level slightly decreased, but still higher than normal control indicting that apoptosis was marked in the 1st month of treatment and its rate started to decline in the 2nd month with more improvement in liver architecture and apoptotic reduction. MAbs-conjugated nanoparticles-treated group showed the most significant improvement results of caspases when compared with other groups in both first and second months of treatment and this revealed its significant improving effect.

Conclusion and recommendations

Dumbell-like nanoparticles conjugated with monoclonal antibodies against both VEGF and cancer stem cell has a targeting effect against hepatocellular carcinoma with the maximum effect at tumor sites not normal tissues as proved by histopathological assessment. Moreover, liver function assays improved significantly with treatment with Dumbell-like nanoparticles conjugated with monoclonal antibodies against both VEGF and cancer stem cell. Although, further studies, including more mice and more investigation, are required, our results could pave the way for a new targeted therapy approach for HCC.

Methods

Reagents and apparatus

Hydrogen tetrachloroaurate (III) hydrate (HAuCl4·3H2O), tetralin, oleylamine tert−butylamine−borane complex (TBAB), acetone, iron pentacarbonyl $Fe(CO)_5$, oleic acid, octadecene, oleylamine, iso-propanol, polyethylene glycol (PEG) diacid, N-Hydroxysuccinimide(NHS), N,N′-dicyclohexylcarbodiimide(DCC), dopamine hydrochloride, chloroform($CHCL_3$), anhydrous Na_2CO_3, hexane, phosphate buffer saline (PBS), hydrogen chloride (HCL), diethylnitrosamine (DEN), and other organic solvents were purchased from Sigma Aldrich (Germany). 1-ethyl-3-(3-dimethyl aminopropyl) carbodiimidewas purchased from Pierce Biotechnology. Dialysis bag (MWCO 10000) was from Fisher while other dialysis bag (MW12,000–14,000 g/mol) was from Serva, Germany. Avastin (bevacizumab) 400 mg/16 ml (Roche, Germany), CD90 monoclonal antibodies was purchased from Miltenyibiotec (130-097-932), sodium chloride 0.9% intravenous infusion (FIPCO), AFP (CanAg EIA kit), caspase-3 (SinogeneclonCo., LTD), VEGF-A (Invitrogen, Thermo fisher Scientific).

Transmitting electron microscopy (JEOLI, JEM-2100), ELISA reader (Biotek), spectroscopy (Cintra), magnetic stirrer and heater (Lab-line instrument), digital balance (AeADAM), centrifuge 5702 R (Eppendorf), pH meter (AD 8000).

I-Preparation of dumbbell-like Au-Fe_3O_4 nanoparticles:

1- **Preparation of Gold nanoparticles**

Gold nanoparticles were purchased from Nanotech Egypt Company for Photo-electronics Dream Land. They were prepared according to Elaidy et al. (2017). Briefly, 0.1 g of hydrogen tetrachloroaurate (III) hydrate (HAuCl4·3H2O) was mixed with tetralin (10 mL), oleylamine (10 mL) then magnetically stirred for 10 min at 10 °C under N_2 flow. A reducing solution of tert−butylamine−borane complex (TBAB), tetralin (1 mL), was mixed then added to the solution. 1 h later at 10 °C, 60 ml of acetone was added to precipitate the Au NPs which collected by centrifugation (8500 rpm for 8 min) then washed and re-dispersed in hexane. The size of the Au particles was tuned by controlling the reaction temperature at 10 °C. The required (8 nm) diameter of Au was checked with transmission electron microscope.

2- **Synthesis of dumbbell-like Au-Fe_3O_4 nanoparticles**

The dumbbell-like Au-Fe_3O_4 nanoparticles were prepared according to Peng et al. (2008) by decomposition of iron pentacarbonyl Fe $(CO)_5$ on the surface of Au nanoparticles followed by oxidation under air. Briefly, 1ml oleic acid and 20 ml octadecene was heated at 120 °C for 20 min in presence of N_2 flow. Then, 0.15 ml Fe $(CO)_5$ and 0.5 ml of oleylamine were added to the solution. 2 ml of previously prepared 8 nm Au colloidal were added and the solution was heated for 45 min (310 °C). Following cooling at room temperature, the particles were separated by addition of iso-propanol, centrifuged and dispersed into hexan. The diameter of Au-Fe_3O_4 was checked with transmission electron microscope.

II-Conjugation of dumbbell-like Au-Fe_3O_4 nanoparticles with monoclonal antibodies:

1- **Surface modification of Au-Fe_3O_4 particles:**

20 mg of PEG diacid, 2 mg of N-Hydroxysuccinimide (NHS), 3 mg of N,N′-dicyclohexylcarbodiimide (DCC) and 1.7 mg of dopamine hydrochloride were dissolved in a mixture solution of $CHCl_3$ (2 mL) and anhydrous Na_2CO_3 (10 mg). The solution was stirred at room temperature for 2 h before adding 5 mg of nanoparticles, and the resulting solution was stirred overnight at room temperature under N_2. The modified nanoparticles were precipitated by adding 5 ml of hexane and collected by a permanent magnet and dried under N_2 then dispersed in PBS. The extra surfactants and other salts were removed by dialysis using a dialysis bag (MWCO 10000) for 24 h in PBS.

2- **Conjugation of Avastin to modified Au-Fe_3O_4 naoparticles:**

A solution of nanoparticles previously dispersed in PBS was mixed with 1-ethyl-3-(3-dimethylaminopropyl) carbodiimide for 15 min. After the addition of Avastin (1mg/ml), the solution was stirred for 1 h and the conjugate was purified by the magnetic separator three times at 4 °C.

3- **Conjugation with CD90 monoclonal antibody:**

Noncovalent conjugation of Au nanoparticles part of the dumbbell Au-Fe_3O_4 nanosystem with CD90 monoclonal antibodies was accomplished by the addition of 170 µg of CD90 to the previously prepared conjugated mixture and kept on sterrier for 30 min.

Images were taken by transmission electron microscopy (JEOLI, JEM-2100) for the synthesized Au-Fe_3O_4 nanosystem before and after conjugation with monoclonal antibodies.

In vitro drug release

One ml of Avastin−Au-Fe_3O_4 was dispersed in de-ionized water then transferred into dialysis bag (cut off molecular weight 12,000–14,000 g/mol, Serva, Germany) with surrounding releasing medium of 50 mL PBS buffer (pH 7.4) and another one ml was dispersed into Tris–HCl buffer (pH 5) dialysis bag at 37 °C. At fixed time intervals, 1 mL of release medium was withdrawn from each dialysis bag release medium then replaced with fresh buffer to maintain

the sink conditions. The amount of released Avastin was determined by UV–Vis spectroscopy at 480 nm. Cumulative drug release percentage was calculated as follows.

$$\text{Cumulative drug release} = \frac{(\text{Amount of Avastin in the release medium})}{(\text{Initial amount of Avastin loaded onto NPs})} \times 100$$

Experimental model

One hundred male Balb/c mice weighing ~ 20 ± 5 gm were enrolled in this study. Animals were raised and maintained at the animal house in TBRI in barrier units with a defined and regularly monitored health status. They were kept under constant temperature and humidity. Mice were fed on a standard diet. The Ethical Committee of experimental animals at TBRI approved the protocols. All guidelines for the care and use of animals were followed, according to IRH of TBRI.

III-Experimental model groups

Mice were divided into five groups:

1- Normal control group: 20 mice were injected *I.P.* with 100 µl saline weekly for 8 weeks.
2- Pathological control group: 20 mice were injected *I.P.* with 200 mg/kg body weight diethylnitrosamine (DEN) diluted in saline once per week for eight consecutive weeks.
3- MAbs-conjugated nanoparticles-treated group: 20 mice were injected *I.P.* with 200 mg/kg body weight diethylnitrosamine (DEN) diluted in saline once per week for eight consecutive weeks then treated with I.V. injection of 100 µl dumbbell nanoparticles conjugated to mAb against both VEGF (Avastin) (400 mg /16 ml) and CD90 (300 µl) every two weeks for 8 weeks.
4- Nonconjugated nanoparticles-treated group: 20 mice were injected *I.P.* with 200 mg/kg body weight diethylnitrosamine (DEN) diluted in saline once per week for eight consecutive weeks then injected *I.V.* with 100 µl of dumbbell nanoparticles alone every two weeks for 8 weeks.
5- Avastin-treated group: 20 mice were injected *I.P.* with 200 mg/kg body weight diethylnitrosamine (DEN) diluted in saline once per week for eight consecutive weeks then treated with *I.V.* injection with 100 µl Avastin every two weeks for 8 weeks.

One animal from each group were scarified after 4 weeks for follow up. After another 4 weeks, residual animals of all groups were sacrificed and sera were analyzed by ELISA technique for AFP, caspases-3, VEGF-A and ALT and AST. Liver sections from sacrificed animals were histopathologically assessed.

IV-Histopathological examination of hepatic specimens

Hepatic specimens were processed and stained with Hematoxylin and Eosin (H & E) for histopathological assessment.

V- Biochemical analysis of collected serum samples:

Commercially available ELISA kits were used to detect HCC markers (AFP), apoptotic markers (caspase-3), and angiogenesis marker (VEGF-A).

Statistical analysis of data

All data are expressed as means and standard deviations. Analysis of variance (ANOVA) and one-way ANOVA were used to analyze within group data and between-group data, respectively. Values of $P \leq 0.05$ will be considered statistically significant.

Abbreviations

HCC	Hepatocellular carcinoma
CD90	Cancer stem cell marker
VEGF	Vascular endothelin growth factor
DEN	Diethylnitrosamine
AST	Aspartate aminotransferase
ALT	Alanine transaminase
ELISA	Enzyme-linked immunosorbent assay
H&E	Hematoxylin and eosin
HBV	Hepatitis B virus
HCV	Hepatitis C virus
CSCs	Cancer stem cells
DBNPs	Dumbbell-like nanoparticles
NPs	Nanoparticles
TEM	Transmission electron microscopy
IP	Intraperitoneal
I.V.	Intravenous

Acknowledgements

Not applicable.

Author contributions

NT, SA, RM, SM, TM, DM and MK wrote the main manuscript text. SA, RM, SM, TM, and MK prepared figures. SA, RM, TM, DM, and MK prepared Tables. WM, SF, NT, and MK supervision. All authors reviewed the manuscript. All authors read and approved the final manuscript.

Funding

Open access funding provided by The Science, Technology & Innovation Funding Authority (STDF) in cooperation with The Egyptian Knowledge Bank (EKB). This work was funded by project 19 K, TBRI, Egypt.

Availability of data and materials

Available.

Declarations

Ethics approval and consent to participate

This work was approved by TBRI ethical committee, Egypt.

Consent for publication

Not applicable.

Competing interests

The Authors declare that they have no competing interests.

Received: 11 November 2022 Accepted: 11 February 2023
Published online: 25 February 2023

References

Akbarzadeh A, Zarghami N, Mikaeili H et al (2012) Synthesis, characterization, and in vitro evaluation of novel polymer-coated magnetic nanoparticles for controlled delivery of doxorubicin. Nanotechnol Sci Appl 5:13–25. https://doi.org/10.2147/NSA.S24328

Alkatout I, Kabelitz D, Kalthoff H et al (2008) Prowling wolves in sheep's clothing: the search for tumor stem cells. Biol-Chem 389:799–811. https://doi.org/10.1515/BC.2008.094

Baharara J, Ramezani T, Divsalar A et al (2016) Induction of apoptosis by green synthesized gold nanoparticles through activation of caspase-3 and 9 in human cervical cancer cells. Avicenna J Med Biotechnol 8:75–83
Baiga B, Abdel Halimb S, Farrukha S et al (2019) Current status of nanomaterial-based treatment for hepatocellularcarcinoma. Biomed Pharma 116:108852. https://doi.org/10.1016/j.biopha.2019.108852
Braghiroli MI, Sabbaga J, Hoff PM (2012) Bevacizumab: Overview of the literature. Expert Rev Anticancer Ther 12:567–580. https://doi.org/10.1586/era.12.13
Bray F, Ferlay J, Soerjomataram I et al (2018) Global cancer statistics 2018: GLOBOCAN estimates of incidence and mortality worldwide for 36 cancers in 185 countries. CA Cancer J Clin 68:394–424. https://doi.org/10.3322/caac.21492
Craig AJ, von Felden J, Garcia-Lezana T et al (2019) Tumor evolution in hepatocellular carcinoma. Nat Rev Gastroenterol Hepatol 2019:1759–5053. https://doi.org/10.1038/s41575-019-0229-4
D'Souza S (2014) A review of in vitro drug release test methods for nano-sized dosage forms. Adv Pharm. https://doi.org/10.1155/2014/304757
d'Angelo I, Parajó Y, Horváth A et al (2010) Improved delivery of angiogenesis inhibitors from PLGA: poloxamer blend micro- and nanoparticles. J Microencapsul 27:57–66. https://doi.org/10.3109/02652040902954729
Elaidy SM, Moghazy A, El-kherbetawy M (2017) Evaluation of the therapeutic effects of polyvinylpyrrolidone-capped silver nanoparticles on the diethylnitrosamine/carbon tetrachloride-induced hepatocellular carcinoma in rats. Egypt J Basic Clin Pharmacol 7:9–24
El-Serag HB (2011) Hepatocellular carcinoma. N Engl J Med 365:1118–1127. https://doi.org/10.1056/NEJMra1001683
Eskens A, Verweij J (2006) The clinical toxicity profile of vascular endothelial growth factor (VEGF) and vascular endothelial growth factor receptor (VEGFR) targeting angiogenesis inhibitors; a review. Eur J Cancer 42:3127–3139. https://doi.org/10.1016/j.ejca.2006.09.015
Gu H, Yang Z, Gao J et al (2005) Heterodimers of nanoparticles: formation at a liquid-liquid interface and particle-specific surface modification by functional molecules. J Am Chem Soc 127:34–35. https://doi.org/10.1021/ja045220h
Han X, Jiang X, Guo L et al (2019) Anti carcinogenic potential of gold nanoparticles synthesized from Trichosanthes kirilowii in colon cancer cells through the induction of apoptotic pathway. Artif Cells Nanomed Biotechnol 47:3577–3584. https://doi.org/10.1080/21691401.2019.1626412
Heddleston JM, Li Z, Lathia JD et al (2010) Hypoxia inducible factors in cancer stem cells. Br J Cancer 102:789–795. https://doi.org/10.1038/sj.bjc.6605551
Hong IS, Jang GB, Lee HY et al (2015) Targeting cancer stem cells by using the nanoparticles. Int J Nanomed 10:251–260. https://doi.org/10.2147/IJN.S88310
Kadkhoda J, Kohal M, Tohidkia M et al (2021) Advances in antibody nanoconjugates for diagnosis and therapy: a review of recent studies and trends. Int J Biol Macromol 185:664–678
Liu G, Yuan X, Zeng Z et al (2006) Analysis of gene expression and chemoresistance of CD133+ cancer stem cells in glioblastoma. Mol Cancer 5:67. https://doi.org/10.1186/1476-4598-5-67
Manghisi G, Elba S, Mossa A et al (1998) A new prognostic system for hepatocellular carcinoma: a retrospective study of 435 patients: the cancer of the liver Italian program (CLIP) investigators. Hepatology 28:751–755. https://doi.org/10.1002/hep.510280322
Nabin P, Vahidfar N, Tohidkia M et al (2021) Mucin-1 conjugated polyamidoamine-based nanoparticles for image-guided delivery of gefitinib to breast cancer. Int J Biol Macromol 174:185–197
Peng S, Lee Y, Wang C et al (2008) A facile synthesis of monodisperse Au nanoparticles and their catalysis of CO oxidation. Nano Res 1:229–234
Qi J, Yao P, He F et al (2010) Nanoparticles with dextran/chitosan shell and BSA/chitosan core—doxorubicin loading and delivery. Int J Pharm 393:176–184. https://doi.org/10.1016/j.ijpharm.2010.03.063
Tapper EB, Parikh ND (2018) Mortality due to cirrhosis and liver cancer in the United States, 1999–2016: observational study. BMJ 362:k2817. https://doi.org/10.1136/bmj.k2817
Xu C, Xie J, Ho D et al (2008) Au-Fe_3O_4 dumbbell nanoparticles as dual-functional. Angew Chem Int Ed 47:173–176. https://doi.org/10.1002/anie.200704392
Yu YH, Chen M, Rice PM et al (2005) Dumbbell-like bifunctional Au-Fe_3O_4 nanoparticles. Nano Lett 5:379–382. https://doi.org/10.1021/nl047955q

Publisher's Note